[This correlation correction reduces the calculated free-electron $J(0)$ by 15%.] The best fits were found for the HF profiles described above: (a) $5\{\text{Ti } 3d^4\}$ and (b) $4\{\text{V } 3d^5\}+1$ free electron. These profiles are shown in Fig. 3 and Table I. Since configuration (a) provides a reasonably good fit to the measured profile, we see, as expected, that in the solid the V band electrons are more spatially extended than in the free atom. The V profile recently calculated by Berggren[13] gives approximately equivalent agreement with the measured $J(z)$.

ACKNOWLEDGMENTS

We thank R. J. Weiss for much helpful advice and Professor C. G. Shull and P. L. Sagalyn for loaning the V crystals.

*Research supported by the National Science Foundation, Grant No. GU-3852.

[1]W. C. Phillips and R. J. Weiss, Phys. Rev. B (to be published).

[2]T. Paakori, S. Manninen, O. Inkinen, and E. Liukkonen, Phys. Rev. B 6, 351 (1972).

[3]R. J. Weiss and J. J. DeMarco, Phys. Rev. 140, A1223 (1965).

[4]W. C. Phillips and R. J. Weiss, Phys. Rev. 171, 790 (1968).

[5]P. Eisenberger and P. M. Platzman, Phys. Rev. A 2, 415 (1970).

[6]R. Currat, P. D. DeCicco, and R. J. Weiss, Phys. Rev. B 4, 4256 (1971).

[7]R. J. Weiss, A. Harvey, and W. C. Phillips, Phil. Mag. 17, 241 (1968).

[8]P. Eisenberger, Phys. Rev. A 5, 628 (1972).

[9]W. A. Rachinger, J. Sci. Instr. 25, 254 (1948).

[10]R. J. Weiss, Phil. Mag. 14, 403 (1966).

[11]R. J. Weiss, *X-Ray Determination of Electron Distributions* (North-Holland, Amsterdam, 1966), p. 185. These calculations employ $3d^n$ wave functions given by R. E. Watson, M.I.T. Solid State and Molecular Theory Group Tech. Rept. No. 12 (1959) (unpublished).

[12]W. C. Phillips and R. J. Weiss, Phys. Rev. B 5, 755 (1972).

[13]K. F. Berggren, Phys. Rev. B 6, 2156 (1972).

PHYSICAL REVIEW B VOLUME 7, NUMBER 3 1 FEBRUARY 1973

Fluctuations in $SrTiO_3$ near the 105-K Phase Transition

Th. von Waldkirch, K. A. Müller, and W. Berlinger
IBM Zurich Research Laboratory, CH-8803 Rüschlikon, Switzerland
(Received 24 July 1972)

The temperature dependence of the EPR linewidth of the Fe^{3+}-V_O pair center in $SrTiO_3$ has been investigated above and below $T_c = 105.6$ K. It is shown from the angular dependence that the pronounced line broadening near T_c results from rotational fluctuations of the oxygen octahedra. The analysis yields a changeover from a fast- to a slow-fluctuation regime for $T \to T_c^+$. The linewidth has a cusp-shaped behavior close to T_c and is finite at T_c. From measurements in samples transforming to monodomains below T_c the anisotropy of the fluctuations is investigated. It is found that they are anisotropic even for temperatures within 10 K *above* T_c, where the point symmetry of the crystal is cubic. In this region, the anisotropy is connected with the increasing regions of correlated motions. Well below T_c it is related to the two distinct soft-mode branches. The results are analyzed in terms of the dynamical form factor $S(\vec{q}, \omega)$. Within a certain approximation they are found to be consistent, for temperatures above and below T_c, with a value of the critical exponent ν (for the correlation length ξ) of $\nu \simeq 0.65$, together with a two-dimensionally anisotropic static-order-parameter susceptibility $\chi(\vec{q}, T)$ with an anisotropy parameter Δ of the order of $\frac{1}{40}$. The changeover from fast- to slow-fluctuation regime yields an estimate of the half-width of the central peak in $S(\vec{q}, \omega)$ of 70 MHz at $T = T_c + 0.8 \pm 0.3$ K.

I. INTRODUCTION

Strontium titanate undergoes a second-order antiferrodistortive phase transition from a cubic to a tetragonal low-temperature phase at $T_c \sim 105$ K, as has been known for a long time.[1-4] This transition is connected with a softening of the threefold-degenerate R_{25} phonon at the R corner ([111] zone boundary)[5,6] and consists of an alternate rotation of nearly rigid oxygen octahedra around one of the $\langle 100 \rangle$ axes. The staggered rotation angle φ is the generalized order parameter of the transition. Many of its static properties have been studied thoroughly,[4,7-10] and static critical phenomena have been observed near T_c in the temperature dependence of the order parameter.[11] In the present paper dynamical properties of the phase transition are investigated using electron paramagnetic resonance (EPR). Recently, it was found that the local rotational fluctuations of the octahedra near T_c can

be probed by the temperature-dependent line broadening of some particular resonances of the Fe^{3+}-V_O pair center.[12,13] This center consists of a trivalent iron impurity with a nearest-neighbor oxygen vacancy.[14] Above T_c the broadening occurs approximately over the same temperature interval[15] over which Riste *et al.*[16] found a central mode with neutron diffraction.

The resonance pattern of a sample containing Fe^{3+}-V_O centers for the static magnetic field $\vec{H}$ in the (001) plane consists above T_c of two mutually perpendicular, highly axial components[14] which belong to centers with axes in the $\vec{H}$ plane along [100] and [010], respectively, and one apparently isotropic resonance near an effective g factor $g^e = 6$ due to the centers with axis along [001]. The effective g factors for the axial spectra vary between $g^e_{\parallel} = 2.0037$ and $g^e_{\perp} = 5.96$ for K-band wavelengths.[17] With $\vec{H}$ in the neighborhood of [110] the axial resonances are highly sensitive to rotational motions of the TiO_6 octahedra. When the sample is cooled down below T_c, where within macroscopic regions (domains) the octahedra are alternately rotated around one of the $\langle 100 \rangle$ axes by the angle φ, they split smoothly into a set of four lines. The low-temperature spectrum has been investigated in detail by von Waldkirch, Müller, and Berlinger[17] (quoted hereafter as I). This work analyzes the influence of the local rotation angle φ_i^{α} at site $\vec{i}$ around the cube axes $\alpha = [100]$, [010], or [001] on the resonance field H_r of the Fe^{3+}-V_O complex for all orientations of the center axis and directions of α and $\vec{H}$. It is found that for $\vec{H}$ near [110] the two inner of the four lines (O and m) belong to centers within domains with rotation axis $\alpha = [100]$ or [010], whereas the two outer ones ($\bar{\varphi}_+$ and $\bar{\varphi}_-$) result from centers within the same domain with rotation axis $\alpha = [001]$ located on the two distinct sublattices rotated by $\pm \varphi^{[001]}$. Hence the split of these two outermost lines is linear in $\varphi^{[001]}$. At 78 K, where $\varphi^{[001]}$ is $1.53° \pm 0.05°$,[4] they are separated by more than 80 G (Fig. 1). Owing to this high sensitivity to local fluctuations in $\varphi^{[001]}$, which for $T \to T_c$ become large, the axial resonance lines broaden. Hence the temperature-dependent linewidth of the axial lines is a good monitor of these fluctuations. A preliminary account of this work emphasizing the information gained for fluctuations around the low-temperature domain axis has been published recently by von Waldkirch, Müller, Berlinger, and Thomas.[13]

In Sec. II the experimental results for several directions of $\vec{H}$ and α in samples transforming to multidomain as well as to monodomain crystals below T_c are reported. Sections III and IV deal with the interpretation of the line broadening above and below T_c, respectively, using a phenomenological theoretical approach, and discuss the refinements of a more detailed analysis. Distinction is made between regimes where the major part of the fluctuations is either fast or slow compared to the characteristic EPR frequency. In Sec. V the observed anisotropy effects are considered, and Sec. VI contains a discussion of the present results and analysis in the light of related experiments.

II. EXPERIMENTAL RESULTS

The experiments were carrie l out on a K-band superheterodyne single-sideband EPR spectrometer. Samples were cut from crystals which were obtained from the National Lead Co. They were grown by the Verneuil flame-fusion technique with 0.03-wt% Fe_2O_3 added to the powder feed. The bulk of the measurements was taken with a plate-shaped sample of $0.3 \times 1.5 \times 5.5$ mm with its long side parallel to the [001] axis and its plane perpendicular to the [110] direction. This choice of coordinate system will be kept throughout the paper. Such samples transform below T_c into a near monodomain with its domain axis, i.e., the c axis (axis of rotation of the TiO_6 octahedra) along [001][18] (see paper I). Confirming measurements have been done on similar $0.3 \times 2 \times 7$-mm samples as used earlier for the static critical effects.[11]

The variable temperatures were maintained by a cold finger attached to the cavity and a direct-current heater (13 Ω at 78 K) wound on the cavity wall. A differential (Au + 2.1-at.% Co)-Cu thermocouple was imbedded in the cavity wall near the heater and its voltage referring to liquid nitrogen compared with an adjustable constant voltage source.[19] The off balance was measured and amplified by a Keithley 149 millimicrovoltmeter and fed through a Hewlett-Packard 6963A power supply to the heater. Owing to the high dc amplification and short delay in temperature between the heater and the thermocouple this proportional stabilization was sufficient. The short-time fluctuations near T_c were about 4 μV at the thermocouple corresponding

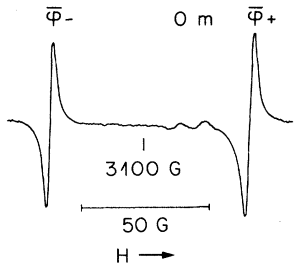

FIG. 1. Split Fe^{3+}-V_O resonance in a well-aligned monodomain $SrTiO_3$ sample with $\vec{H}$ along [110] at 78 K. The measuring frequency is 19.34 GHz. The dominant domain c axis lies along [001], corresponding to $\bar{\varphi}_-$ and $\bar{\varphi}_+$ lines. The O and m lines result from centers within remainders of different domains. See Ref. 17.

to a maximum temperature variation of 0.1 K. However, the variations in the crystal centered in the cavity were at least one order of magnitude smaller. We could easily observe EPR absorptions in $SrTiO_3$ crystals without any signal change during 10 min due to frequency pulling, although this material is known for its high and strongly temperature-dependent dielectric constant.

For the first set of data the sample was oriented with its long basis parallel to the rotation axis of the scanning magnet, i.e., $\vec{H}$ lies in the (001) plane. The temperature dependence of the linewidth ΔH as given by the peak-to-peak separation of the absorption derivative for $\vec{H}$ 0.3° from [110] is shown in Fig. 2(a). The exact [110] direction for $\vec{H}$ was avoided because there the two mutually perpendicular resonances cross at $g^e \simeq 4.5$. When $\vec{H}$ is rotated out of [110] by 0.3° they are separated by about 30 G. Close to T_c, where the linewidth becomes large, sufficient separation was obtained for $\vec{H}$ 0.7° from [110]. Figure 2(a) refers to the lower field resonance for $T > T_c$. Below T_c both resonances are split into two lines, $\bar{\varphi}_+$ and $\bar{\varphi}_-$ (I) (cf. Fig. 1), and the measurements of Fig. 2(a) have been made for the lowest field line. It is seen that $\Delta H(T)$ exhibits a significant increase over a "regular" background for $T \to T_c$ from both sides. Since for a few degrees below T_c the line shape is asymmetric[20] and, close to T_c^-, the two lines overlap, the linewidth is difficult to define within about 2 K below T_c.

To make sure that the broadening effect is caused directly by rotational fluctuations and not indirectly by a critical shortening of T_1 relaxation time,[21] the temperature-dependent line broadening has also been measured for the apparently isotropic line at $g^e \simeq 6$ with $\vec{H}$ along [110]. This resonance is known to be entirely insensitive to rotational motions (see Fig. 6 of I), correspondingly, it is not broadened by rotational fluctuations. The result is displayed in Fig. 2(b). The fact that within the experimental error no extra broadening occurs near T_c indicates that a critical T_1 relaxation contribution for this line at $g^e \simeq 6$ is not observed. Assuming the broadening of Fig. 2(a) to result from a critical T_1 process would then imply a very large anisotropy in T_1 of about 1:15 from Figs. 2(a) and 2(b) which has never been reported for Fe^{3+} ions even in strongly anisotropic coordination.[22] Furthermore, if a T_1 process became dominant on approaching T_c, it would not be understandable why the lines become Gaussian for $T \to T_c^+$ and asymmetric for $T \to T_c^-$.[20]

In I it is found that the axial line investigated is linearly split by $\varphi^{[001]}$ with a comparatively small shift proportional to $(\varphi^{[001]})^2$ for $\vec{H}$ in the (001) plane between about 10° and 60° from [100]. The $\varphi^{[010]}$ component enters only quadratically and the $\varphi^{[100]}$ component is entirely ineffective. The influence of the quadratic contributions to the broadening at T_c for $\vec{H}$ near [110] may be estimated from I to be of the order of a few percent of the maximum linear $\varphi^{[001]}$ effect. The quadratic contributions can be probed separately by the broadening of the apparently isotropic $g^e \simeq 6$ line (see I) with $\vec{H}$ close to [100]. There the line, which is completely insensitive to $\varphi^{[001]}$, shows quadratic shifts by $\varphi^{[010]}$ and $\varphi^{[100]}$ of practically the same magnitude as for the axial lines with $\vec{H}$ near [110]. This line broadens only by approximately 0.8 G at T_c. Compared to the broadening of the axial line [Fig. 2(a)], this

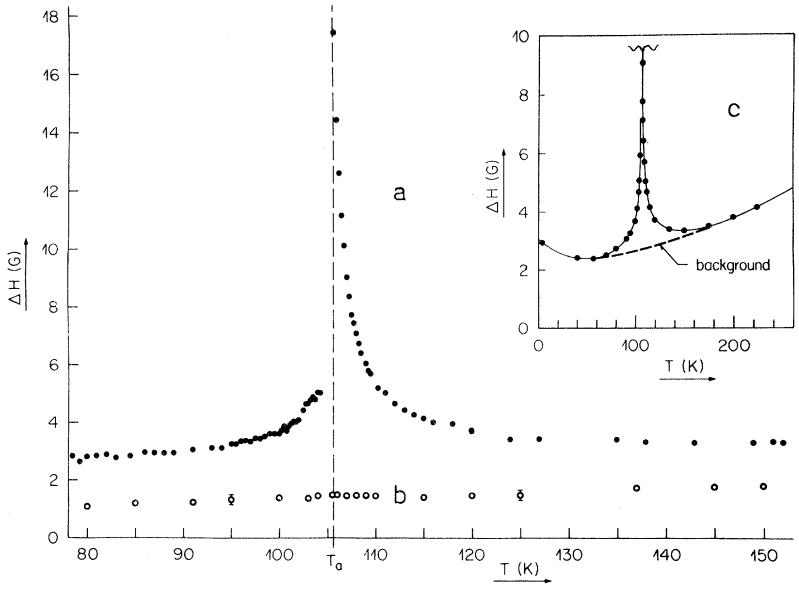

FIG. 2. Observed linewidth broadening of the Fe^{3+}-V_O resonance at the structural phase transition of $SrTiO_3$ for $\vec{H}$ along 0.3° from [110] in the (001) plane, $\vec{c} \parallel [001]$ at 19.2 GHz. (a) For the axial line at $g^e = 4.5$. Below T_c, the measurements refer to the $\bar{\varphi}_-$ line. (b) For the $g^e = 6$ line. (c) Determination of the background width.

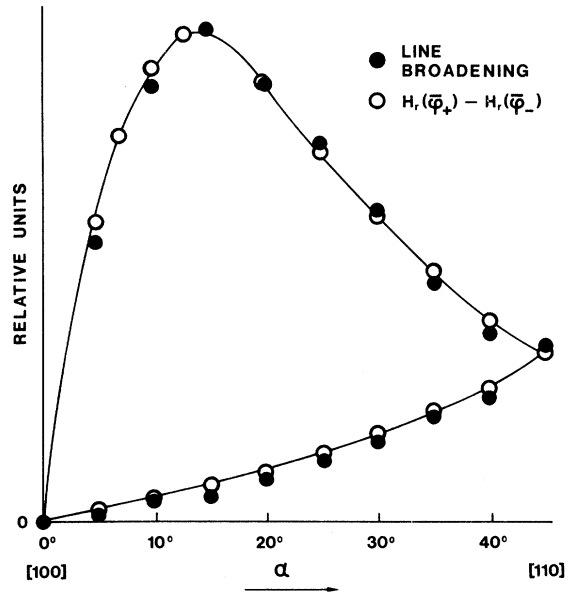

FIG. 3. Comparison between the angular dependences of the broadening of the axial Fe^{3+}-V_O line at $T_c + 0.5$ K and the split between $\bar{\varphi}_+$ and $\bar{\varphi}_-$ lines at 78 K for $\vec{H}$ in the (001) plane, including the theoretically calculated splitting (solid lines). The background width, assumed isotropic, has been subtracted from the experimental linewidth.

confirms the theoretical estimate. Hence, the quadratic broadening effect for the broadening of Fig. 2(a) may be neglected.

The neglect of critical T_1 relaxation as well as quadratic fluctuation effects is further confirmed by the angular variation of the linewidth of the axial line for $T = T_c + 0.5$ K with $\vec{H}$ in the (001) plane. If the line is linearly broadened by the rotational $\varphi^{[001]}$ fluctuations, the angular variation of the linewidth corrected for the background width (which has been assumed isotropic for $T > T_c$) should follow the angular dependence of the linear split of the line by the fixed nonzero value of $\langle \varphi^{[001]} \rangle$ at $T < T_c$. This comparison is shown in Fig. 3, where the circles represent the splitting of the line into $\bar{\varphi}_+$ and $\bar{\varphi}_-$ at 78 K. The solid line represents the theoretical curve for the splitting between $\bar{\varphi}_+$ and $\bar{\varphi}_-$ calculated from I. The expected agreement is seen to be very good.

When the temperature dependence of the linewidth with the same experimental arrangement is measured in a sample which below T_c transforms into a multidomain, a different behavior is found. Within a few degrees above T_c the resonance line is composed of a relatively narrow line with shoulders of about the width observed in the monodomain sample. This is an indication that for $T \to T_c^+$ within the increasing regions where the rotational fluctuations are correlated in the sense of the low-temperature phase they are no longer isotropic for all three φ^α components. This anisotropy of the fluctuations can again be measured directly in the sample transforming to a monodomain. Figure 4 shows the temperature dependence of the linewidth of the axial line with $\vec{H}$ parallel to $[101] - 0.5°$ (again the lower field line) when $\vec{H}$ rotates in the (010) plane (denoted by φ_a). This line is insensitive to $\varphi^{[001]}$ components, since it belongs

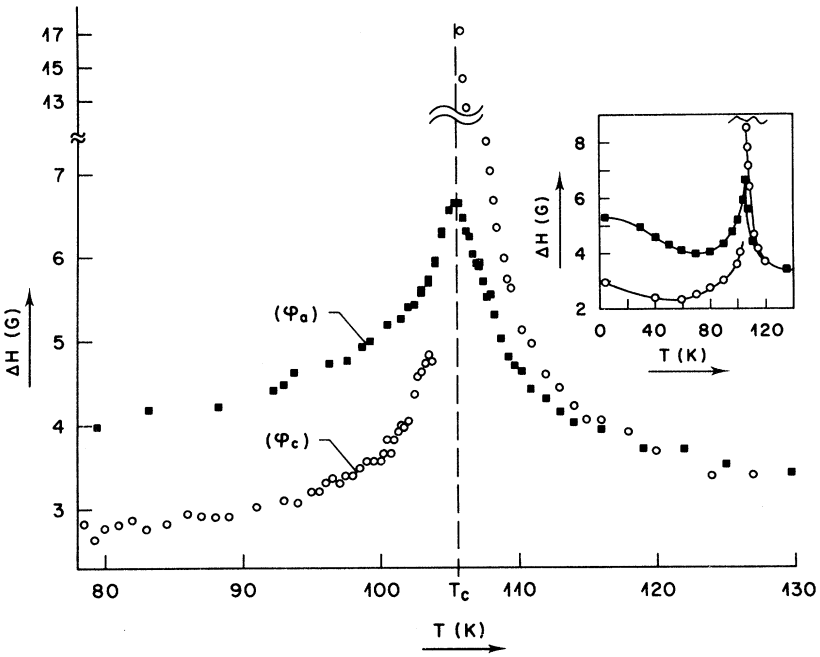

FIG. 4. Anisotropy of the temperature-dependent linewidth in a monodomain sample with $\vec{c} \parallel [001]$. Circles represent data reproduced from Fig. 2(a), denoting broadening caused by fluctuations around the c axis. Squares are measured for the corresponding line with $\vec{H}$ along 0.5° from [101] and represent broadening by fluctuations around an a axis.

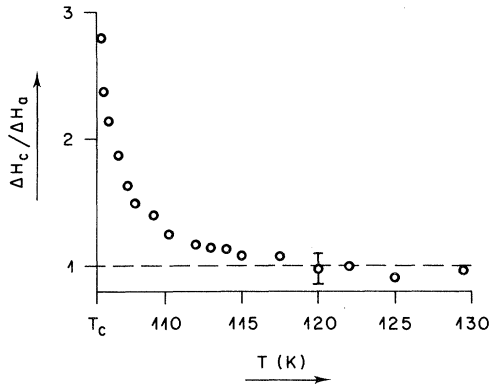

FIG. 5. Ratio of the linewidths induced by φ_c-type (ΔH_c) and φ_a-type (ΔH_a) fluctuations as a function of temperature above T_c. The first three points above T_c are calculated by quadratic, the others by linear subtraction of the background.

to a center with axis parallel to [001] (see I) but it is linearly sensitive to $\varphi^{[010]}$ fluctuations. For comparison, part of the data of Fig. 2(a) is reproduced in Fig. 4 and denoted by φ_c. For $T < 115$ K, the linewidth starts to be anisotropic, indicating that the fluctuations are no longer isotropic. The maximum ratio of the widths of the φ_c and φ_a broadened lines corrected for the background, is of the order of 3 (Fig. 5). Moreover, the temperature dependence of ΔH for the φ_a-broadened line is more symmetric with respect to T_c. For temperatures well below T_c the anisotropy is qualitatively connected with the loss of cubic symmetry of the crystal.

This difference in line broadening for $T \geq T_c$ explains the results obtained in "multidomain" samples and the weak shoulders observed. They are the result of the superposition of a small and a broad line due to regions correlated with respect to [010] or [100] and to [001] rotational fluctuations, respectively.

III. INTERPRETATION FOR $T \geqslant T_c$

A. Phenomenology of the Fluctuation Spectrum

As pointed out in Sec. II the axial EPR resonance line with $\vec{H}$ along [110] [see Fig. 2(a)] is broadened by the *local* fluctuations of the Fe^{3+}-V_O pair-center axis. Only the rotational changes around the [001] crystal axis are significant. This broadening thus reflects the temperature behavior of the spectrum of the local variable $\phi_{\vec{l}}^{[001]}$ denoting the instantaneous angle between the center axis and its average direction. For $T \geq T_c$ the latter is parallel to [100]. The angle $\phi_{\vec{l}}^{[001]}$ results from the rotations of the oxygen complex by $\varphi_{\vec{l}}^{[001]}$ and from the motions of the Fe^{3+} ion. Both contributions are random functions, but only the spectrum of $\varphi_{\vec{l}}^{[001]}$ will show a critical temperature dependence at the phase transition. This spectrum is contained in the local correlation function at site $\vec{l}$: $\langle \varphi_{\vec{l}}^{[001]}(t)\varphi_{\vec{l}}^{[001]}(0)\rangle$. Since in $SrTiO_3$ the phase transition occurs with respect to the collective motion at $q_R = (\frac{1}{2}, \frac{1}{2}, \frac{1}{2}) \times (2\pi/a)$[3-6] we Fourier-transform in space to the staggered collective coordinates with q origin at q_R: $\varphi_{\vec{q}}^{[001]}(t) = \sum_{\vec{l}} e^{-i(\vec{q}+\vec{q}_R)\cdot\vec{l}}\varphi_{\vec{l}}^{[001]}$. The Fourier transform in time of the staggered correlation function is the dynamic form factor

$$S(\vec{q}, \omega) = (1/2\pi)\int_{-\infty}^{+\infty} \langle \varphi_{\vec{q}}(t)\varphi_{-\vec{q}}(0)\rangle e^{i\omega t}\, dt\,, \qquad (1)$$

where the indices [001] have been omitted for simplicity.

Experimental information on the dynamic form factor can be obtained by inelastic neutron and Raman scattering.[23] The scattered intensity is directly proportional to $S(\vec{q}, \omega)$. Earlier investigations by Fleury, Scott, and Worlock[5] (for $T \leq T_c$) and Shirane and Yamada[6] have revealed the existence of the soft-phonon modes around q_R, manifesting themselves in well-defined peaks at $\pm\omega_s(\vec{q})$ in $S(\vec{q}, \omega)$. This finding was along the line of the general theory of soft-phonon-driven phase transitions and especially discussed in a paper by Cochran and Zia,[24] who had pointed out the possibility of a soft R_{25} corner mode in several perovskite crystals. Slonczewski and Thomas[25] and Pytte and Feder[26] have given detailed theoretical explanations in terms of a Landau potential and in a mean-field microscopic treatment for the particular R_{25} soft-phonon behavior in $SrTiO_3$. These investigations, based on a note by Thomas and Müller,[27] quantitatively emphasize the direct relationship between the soft phonons in $SrTiO_3$ and $LaAlO_3$ which transforms to a trigonal structure below T_c. Experimentally, this relationship was further demonstrated by the pressure-induced trigonal phase in $SrTiO_3$.[28] Recently, for $T \geq T_c$, $S(\vec{q}, \omega)$ has been reinvestigated with neutron scattering by Riste *et al.*[16] They found that for temperatures up to the order of 40 K above T_c, $S(\vec{q}, \omega)$ not only reveals two soft-mode resonances at $\omega = \pm\omega_s$ but also a sharp "central peak" around $\omega = 0$ which for $T \to T_c^+$ becomes dominant. $S(\vec{q}, \omega)$ is thus characterized by three poles.

The dynamic form factor $S(\vec{q}, \omega)$ is given by the general expression[29-31]

$$S(\vec{q}, \omega) = \frac{1}{\pi} k_B T \chi(\vec{q}, \epsilon) \times \frac{\omega_0^2(\vec{q}, \epsilon)\Gamma'(\vec{q}, \omega)}{[\omega^2 - \omega_0^2(\vec{q}, \epsilon) + \omega\Gamma''(\vec{q}, \omega)]^2 + [\omega\Gamma'(\vec{q}, \omega)]^2}\,, \qquad (2)$$

where $\chi(\vec{q}, \epsilon)$ denotes the temperature-dependent static-order-parameter susceptibility of $\varphi_{\vec{q}}^{[001]}$ with $\epsilon \equiv (T - T_c)/T_c$; $\omega_0(\vec{q}, \epsilon)$ is a temperature-depen-

dent characteristic frequency related to $\chi(\vec{q}, \epsilon)$ by

$$\omega_0^2(\vec{q}, \epsilon) \propto 1/\chi(\vec{q}, \epsilon) , \tag{3}$$

and $\Gamma(\vec{q}, \omega) = \Gamma'(\vec{q}, \omega) + i\Gamma''(\vec{q}, \omega)$ is a complex damping function. Equation (2) contains the relation

$$\int_{-\infty}^{+\infty} S(\vec{q}, \omega)\, d\omega = k_B T \chi(\vec{q}, \epsilon) \tag{4}$$

derived by application of the fluctuation-dissipation theorem and the Kramers-Kronig relations. Recently, Schwabl[31] gave a phenomenological treatment of the dynamic form factor above the phase transition. The desired three-pole structure of $S(\vec{q}, \omega)$ with its characteristic temperature behavior is obtained from Eq. (2) by the phenomenological *Ansatz*[31,32]

$$\Gamma(\vec{q}, \omega) = \delta^2(\vec{q})/[\lambda(\vec{q}) + i\omega] + \sigma. \tag{5}$$

In this expression the parameters $\delta(\vec{q})$, $\lambda(\vec{q})$, and σ are taken to be uncritical near T_c. From Eqs. (2), (3), and (5) it is seen that the specific temperature behavior of $S(\vec{q}, \omega)$ near T_c is given by the divergence of $\chi(\vec{q}, \epsilon)$.[33] Schwabl[31] assumes an anisotropic Ornstein–Zernike type susceptibility for rotations of the oxygen octahedra around $\alpha = [100]$, $[010]$, or $[001]$:

$$\chi(\vec{q}, \epsilon) = \chi_0[\vec{q}^2 - (1 - \Delta)q_\alpha^2 + \kappa^2]^{-1+\eta/2} . \tag{6}$$

Here χ_0 contains the single-particle susceptibility, and $\kappa(\epsilon) = \kappa_0 \epsilon^\nu$ is the inverse of the correlation length $\xi(\epsilon)$. ν and η are critical exponents,[23] the latter describing the deviation from classical Ornstein–Zernike behavior on ϵ. q_α denotes that component of the q space, which corresponds to the rotation axis α of the fluctuations under consideration. The parameter Δ takes into account the possible anisotropy of the dispersion of $\chi(\vec{q}, \epsilon)$ near $\vec{q}_R$. This is an important new refinement since for rotations around a certain axis α, the in-plane coupling of the oxygen octahedra by common corners is large compared to the interplane coupling. From Eqs. (2) and (3) one obtains for the static part

$$S(\vec{q}, \omega = 0) = (1/\pi) k_B T \chi(\vec{q}, \epsilon) \omega_0^{-2} \Gamma'(\vec{q}, \omega = 0)$$

$$\propto \Gamma'(\vec{q}, \omega = 0) T \chi^2(\vec{q}, \epsilon) \quad . \tag{7}$$

B. Influence of Fluctuations on Linewidth

The T_1 relaxation effect has been seen to be negligible, apparently because the rotational motion even for a Raman process couples negligibly for our system. As shown in Sec. II, from the analysis of the Fe^{3+}-V_O spectrum below T_c it is deduced that for the experimental arrangement used with $\vec{H}$ close to [110] the resonance magnetic field H_r depends linearly on $\varphi_{\vec{l}}^{[001]}$ (Ref. 34):

$$H_r(t) = H_0 + A\varphi_{\vec{l}}^{[001]}(t) = H_0 + A\sum_{\vec{q}} e^{+i(\vec{q}+\vec{q}_R)\cdot\vec{l}} \varphi_{\vec{q}}^{[001]} , \tag{8}$$

where $A = 26$ G/deg (see Paper I). Hence the departure δH from H_0 is a random function proportional to $\varphi_{\vec{l}}^{[001]}(t)$. The probability distribution of $\delta H(t)$ is assumed to be Gaussian. The situation therefore is analogous to the problem of NMR linewidth in the presence of motion of the nuclei treated by Abragam.[35] The second moment of the line is proportional to the temperature-dependent mean-square value of the fluctuations and is unaffected by the motion. It is given by

$$\langle \delta H^2 \rangle = A^2 \langle (\varphi_{\vec{l}}^{[001]})^2 \rangle = A^2 \langle \varphi_{\vec{l}}^{[001]}(t) \varphi_{\vec{l}}^{[001]}(t) \rangle$$

$$\propto \sum_{\vec{q}} \int_{-\infty}^{+\infty} S(\vec{q}, \omega)\, d\omega . \tag{9}$$

As long as $S(\vec{q}, \omega)$ contains only frequencies low compared to the characteristic frequency ω_m, $2(\langle \delta H^2 \rangle)^{1/2}$ will represent the experimental linewidth ΔH, and the line shape will be Gaussian as the distribution of $\varphi_{\vec{l}}^{[001]}$. The frequency ω_m is of the order of the instantaneous spread in Larmor frequency over the crystal owing to the distribution of $\varphi_{\vec{l}}^{[001]}$, which at T_c is of the order of the maximum linewidth. Thus $\omega_m/(2\pi)$ at T_c is estimated to be of the order of 10^8 sec^{-1}. Since the instantaneous spread in $\varphi_{\vec{l}}^{[001]}$ is by itself temperature dependent, ω_m will also be a function of temperature. With increasing $|\epsilon|$ it decreases. [At the same time the width of the central peak in $S(\vec{q}, \omega)$ increases.] Then $S(\vec{q}, \omega)$ contains frequencies large compared to $\omega_m(T)$, and only the quasi-adiabatic components of $S(\vec{q}, \omega)$ will contribute to the broadening, since all faster components are averaged to zero. In this case the line will be narrower than in the case of a rigid lattice with a width $\Delta H < 2(\langle \delta H^2 \rangle)^{1/2}$. This effect is known as motional narrowing.

Denoting by $\omega_1(T)$ the frequency equivalent of the linewidth $\Delta H(T)$ all components of $S(\vec{q}, \omega)$ within $\pm\omega_1$ will contribute to the broadening. This yields for the fast-fluctuation case the implicit equation for ΔH[35]

$$\Delta H^2 \sim \sum_{\vec{q}} \int_{-\omega_1}^{\omega_1} S(\vec{q}, \omega)\, d\omega . \tag{10}$$

In the limit where ω_1 can be regarded as so small compared to the frequency dependence of $S(\vec{q}, \omega)$ around $\omega = 0$ that $S(\vec{q}, \omega) \simeq S(\vec{q}, \omega = 0)$ within $\pm\omega_1$, Eq. (10) can be rewritten

$$\Delta H \sim \sum_{\vec{q}} S(\vec{q}, \omega = 0) . \tag{11}$$

The detailed analysis of Abragam[35] and Schwabl[31] yields that in this case of fast fluctuations the line shape is Lorentzian rather than Gaussian as in the slow-motion regime. The implications of the changeover from the fast to the slow-motion regime as discussed recently by Rigamonti[36] are described in the last paragraph of Sec. III.

C. Application to Experimental Results: Fast-Motion Regime

To isolate the extra broadening near T_c due to the rotational fluctuations $\varphi_i^{[001]}(t)$ the experimental linewidths have to be corrected for the background width resulting from strains, relaxations, and different mode fluctuations. This background is by itself temperature dependent and has been interpolated as indicated in Fig. 2(c). The line shape of the background resonance is close to Lorentzian as determined by a least-squares fit at 150 K.[37]

Well above T_c the fluctuations are fast, yielding an essentially Lorentzian extra broadening. Its width is therefore obtained from the measured width by linear subtraction of the background. Neglecting the q dependence of Γ' it follows from Eqs. (11) and (7) that

$$\Delta H \propto T \sum_{\vec{q}} \chi^2(\vec{q}, \epsilon) . \tag{12}$$

Since all collective coordinates $\varphi_{\vec{q}}^{[001]}$ with wave vector $\vec{q}$ within the first Brillouin zone represent *rotational* motions of the oxygen octahedra, the sum in Eq. (12) runs over all these $\vec{q}$ values. For $\chi(\vec{q}, \epsilon)$ the modified Ornstein–Zernike expression (6) proposed by Schwabl[31] may be used. Although this expression is the dominant contribution to the susceptibility in a limited $\vec{q}$ range only, for determination of the temperature behavior of ΔH it may be used as an approximation within the entire Brillouin zone since the corrections for larger $\vec{q}$ values are uncritical near T_c and their contribution is hence contained in the background. Taking for the single-particle susceptibility χ_s a Curie-law behavior in analogy to magnetic and liquid systems, and assuming χ_0 in Eq. (6) to be directly proportional to χ_s yields $\chi_0 \propto 1/T$. The latter assumption means that we neglect the temperature dependence of the parameter R^2 in the general Ornstein–Zernike expression.[23]

The leading contribution to the linewidth near T_c within this approximation is then obtained from Eq. (12)[31]:

$$\Delta H \propto [\kappa(\epsilon)^{-(1-2\eta)}/T\sqrt{\Delta}\,] \arctan[\pi\sqrt{\Delta}/\kappa(\epsilon)\,a] , \tag{13}$$

where $a = 3.9$ Å is the lattice constant. From this it is seen that close enough to T_c when $\epsilon < (\pi\sqrt{\Delta}/\kappa_0 a)^{1/\nu}$ the linewidth behaves as

$$\Delta H \propto \epsilon^{-\nu(1-2\eta)} . \tag{14}$$

For higher temperatures we obtain with $\arctan x \sim x$,

$$\Delta H \propto \epsilon^{-\nu(2-2\eta)} . \tag{15}$$

The range of validity of these two relations is determined by the value of the anisotropy parameter Δ. Fitting the experimental points to expression (13) also in the temperature range from 105.75 to 106.5 K would require $T_c \sim 104.5$ K. However, given a second-order phase transition, T_c is experimentally defined at 105.6 ± 0.15 K where the order parameter (splitting of the line) vanishes,[11] coinciding with the maximum of the linewidth. Thus for $T \to T_c^+$ the linewidth does not diverge as the fast-fluctuation formula (13) indicates. For temperatures between $T_c + 1$ K and $T_c + 10$ K, where the "reduced" linewidth depends very slightly on the choice of background, the curvature of the log-log plot (Fig. 6) does not allow an independent determination of ν and Δ. The mean slope of the curve of Fig. 6 in this region corresponds to a value of $\nu = 0.74 \pm 0.03$ in Eq. (14). η is set equal to zero as it is estimated to be of the order of the experimental error. This value of ν compares well with the one found by Riste *et al.*[16] from neutron scattering. However, this value of ν is not consistent with that of $\beta = 0.33 \pm 0.02$ determined by Müller and Berlinger[11] by EPR, and with $\gamma' = 1.29 \pm 0.10$ calculated by Schneider and Stoll[38] using the observed changeover from $\beta \simeq \frac{1}{2}$ outside the critical region, to $\frac{1}{3}$ near T_c.[11] Assuming the static scaling hypothesis[23] to be valid, $\gamma = \gamma'$, and the above values of the critical exponents together with $\alpha \sim 0$, the scaling relation $\alpha + 2\beta + \gamma = 2$ is nicely obeyed. Hence β and γ are consistent amongst each other. From the relation[23]

$$(2 - \eta)\nu = \gamma , \tag{16}$$

with $\eta = 0$ we would then expect for ν a value near 0.65 rather than 0.74. Starting from $\nu = 0.65$ in Eq. (13) we arrive at an anisotropy parameter Δ of 0.02 ± 0.01. This fit, as obtained on an IBM 1130 computer with a 2250 display unit, is shown in Fig. 6. κ (115 K) = 0.05 Å^{-1} was taken from the determination by neutron diffraction by Riste *et al.*[16]

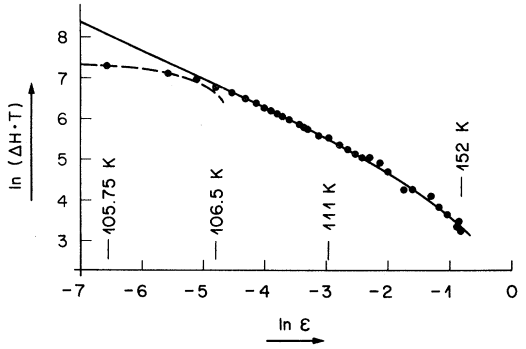

FIG. 6. Comparison between experimental and theoretical φ_c-broadened linewidths for the fast- and slow-motion regimes for $T \geq T_c$. For the latter, the theoretical curve shows $(\langle \Delta H^2_{\text{crit}} \rangle)^{1/2}$; for convenience it is adapted to the experimental points determined by linear subtraction of the background width, as in the fast-motion regime. •, experimental data; solid line, theory fast; dashed line, theory slow.

In the recent extensive account of their work[39] these authors indicate an error for κ (115 K) of $\pm 40\%$, resulting in an additional uncertainty in Δ of $+100\%$ and -60%. Assuming Eq. (13) to remain valid also for higher temperatures ν and Δ can be determined independently by a fit of Eq. (13) to the experimental points in a somewhat larger temperature region.[13] For temperatures up to 152 K (Fig. 6) one obtains $\nu = 0.63 \pm 0.07$ and $\Delta = 0.02 \pm 0.015$. Hence, including the error in κ (115 K), it may be implied from experiment and with the arguments above that $\nu = 0.65 \pm 0.05$ with Δ of the order of $\frac{1}{40}$. This value of the anisotropy parameter Δ means that roughly 40 octahedral units in a (001) plane are correlated when one in a next (001) plane is correlated to them in the sense of the $I4/mcm$ structure. This is understood qualitatively by the strong gearlike in-plane coupling between the alternately rotating oxygen octahedra as compared to the weak coupling through the oxygen ions between the planes. A comparison between the anisotropy determined here and the one observed in soft-mode dispersion around q_R by neutron scattering[40] will be given in Sec. VI.

As pointed out by Stanley,[41] the particular rotational mode of the oxygen octahedra together with the "pancake"-type correlations with definite rotation axis found here in the cubic phase may, to a certain extent, be compared to the behavior of the planar Heisenberg model.[23] The "spin" direction is, for instance, defined by the corresponding Ti-O junction lines. The comparison is still limited by the fact that for mechanical reasons the rotational angle of the octahedra is bounded to within a few degrees, hence the "spins" may not rotate all round. Furthermore, the interactions are nonuniform; this causes the anisotropic correlation, but appears to have little effect on the critical exponents.[23] However, the anisotropy is coupled with the direction of the "spins," i.e., with the axis of rotation. A phase transition of the planar Heisenberg type is therefore more closely related to a crystal which, owing to shaping, transforms into a monodomain, i.e., the rotations and fluctuations of the octahedra are anisotropic even above T_c (Sec. V). This model[23] yields critical exponents $\beta = \frac{1}{3}$, $\gamma = \frac{4}{3}$ and $\nu = \frac{1}{2}\gamma = \frac{2}{3}$ with $\eta = 0$. These values agree well with the experimentally deduced values cited above.

D. Slow-Motion Regime

For temperatures below 106.5 K the fast-fluctuation regime described by Eq. (13) is seen to be no longer valid (Fig. 6). The nondivergent width is expected since ΔH is a local variable not depending on the volume of the system considered and hence not sensitive to the divergence of correlated regions.[42] Furthermore, the mechanical coupling between the rotating oxygen octahedra at most allows a maximum local value of $\varphi_{\vec{1}}^{[001]}$ of the order of $\langle \varphi_{\vec{1}}^{[001]} \rangle$ $(T=0) \sim 2°$.[4] The latter fact prevents $\langle (\varphi_{\vec{1}}^{[001]})^2 \rangle$ from diverging for $T \to T_c$, where $\langle (\varphi_{\vec{1}}^{[001]})^2 \rangle$ means the ensemble average of the square of the local fluctuations $\varphi_{\vec{1}}^{[001]}$.

On approaching T_c the fluctuations are critically slowed down and their oscillator strength is more and more concentrated in the central peak,[16,30,31] which contains only frequencies very close to zero. Its width narrows to zero for $T \to T_c$, and hence close enough to T_c the fluctuations are concentrated at frequencies low compared to the characteristic measuring frequency ω_m. In this "slow-motion regime" therefore the line reflects instantaneous behavior and is inhomogeneously broadened. It is then essentially characterized by a Gaussian line shape.[31,35] The change from Lorentzian to more Gaussian-type resonances is found experimentally. A least-squares fit of the resonance line (which effectively is a convolution of the Lorentzian background and Gaussian "critical" broadening) to a sum of Lorentzian and Gaussian lines yields 50% Gaussian at $T_c + 1.5$ K. The "critical" broadening given by the deconvolution of the resonance line may approximately be obtained in this case by quadratic subtraction of the background width:

$$\Delta H_{\text{crit}}^2 \simeq \Delta H_{\text{expt}}^2 - \Delta H_{\text{background}}^2 \,. \tag{17}$$

From Sec. III B we then have

$$\Delta H_{\text{crit}}^2 = 4 \langle \delta H^2 \rangle \propto \int_{q=0}^{\pi/a} \int_{\omega=-\infty}^{+\infty} S(\vec{q}, \omega) d^3q \, d\omega \,, \tag{18}$$

where $S(\vec{q}, \omega)$ is dominated by the central peak. From Eq. (4) this yields

$$\Delta H_{\text{crit}}^2 \propto T \int_0^{\pi/a} \chi(\vec{q}, \epsilon) \, d^3q \,. \tag{19}$$

This result is verified from Eq. (2) by extraction of the central peak. It is obtained by expansion for small frequencies in the limit $\sigma \ll \delta^2/\lambda$, yielding a Lorentzian of width $\omega_0^2\gamma/(\omega_0^2 + \delta^2)$.[30-32] The frequency-integrated intensity of the central peak in the critical limit $\omega_0^2 \to 0$ for $T \to T_c$ again yields Eq. (19). Inserting Schwabl's expression (6) for $\chi(\vec{q}, \epsilon)$ into Eq. (19) with $\eta = 0$ yields for the critical contribution ($\kappa \to 0$), using cylinder coordinates:

$$\Delta H_{\text{crit}}^2(\epsilon) \propto \text{const} - [\kappa(\epsilon)/\sqrt{\Delta}] \arctan[\pi\sqrt{\Delta}/\kappa(\epsilon)a] \,. \tag{20}$$

The second term which for $\kappa \to 0$ becomes linear in κ, vanishes at $T = T_c$ so that the first term describes the *finite* maximum width at the phase transition. Close to T_c, where $(\pi\sqrt{\Delta})/[\kappa(\epsilon)a] \gg 1$, Eq. (20) is rewritten

$$\Delta H_{\text{crit}}^2(\epsilon) = \Delta H_{\text{max}}^2 (1 - C\epsilon^{\nu}) \,, \tag{21}$$

where C is a proportionality constant. From a best

fit to the experiments we obtain $\Delta H_{max} = 19.7$ G and $C = 18.6$. However, because the validity range of the slow-motion limit is not determined, these values, especially C, may be somewhat uncertain. Since the critical contribution to $\langle \varphi_{\vec{1}}^2 \rangle$ comes from the small wave-number part in $S(\vec{q}, \omega)$ only, the drop from 19.7 to about 15 G in the slow-motion regime may appear fairly large. On the other hand, the central peak is concentrated at small q values, and $S(\vec{q}, \omega)$ for larger q values is hence dominated by high frequencies, which do not contribute to the broadening. Therefore, the small-wave-number part of $S(\vec{q}, \omega)$ is strongly weighted by the experiment. This justifies also the use of the Ornstein–Zernike type expression (6) for the static susceptibility. In this region the experimental uncertainties of T_c and ΔH_{max}^{expt} do not allow an accurate independent determination of the exponent ν. Therefore, $\nu = 0.65$ has been taken from the first analysis. The value of ΔH_{max} derived from Eq. (21) lies well within the experimental error. The theoretical curve according to this regime is included in Fig. 6. The result of Eq. (21) shows that for $T \to T_c^+$ the linewidth has a cusp-shaped behavior.[23]

From Eqs. (8), (9), and (18) an experimental value for $\langle (\varphi_{\vec{1}}^{[001]})^2 \rangle^{1/2}$ at T_c is derived of 0.4° which is about 20% of $\langle \varphi_{\vec{1}}^{[001]} \rangle$ at $T = 0$ K. It is in remarkably close agreement with the value of the generalized order parameter $\langle \varphi_{\vec{1}}^{[001]} \rangle$ near 100 K where the deviation from Landau behavior in the temperature dependence of the order parameter is observed.[11] Since the deviation to critical behavior is expected when the fluctuations for $\vec{q} = 0$ become of the same order as the order parameter, and the present experiment is particularly sensitive to fluctuations at small wave numbers, such agreement is in accordance with expectation.

E. Changeover Between Fast- and Slow-Motion Regimes

The changeover from the fast- to the slow-fluctuation regime is found between 106 and 107 K (Fig. 6). Dynamically, it is characterized by the fact that the local fluctuations start to contain essentially only frequencies low compared to the characteristic frequency ω_m given by the instantaneous spread in Larmor frequency. Since $\omega_m(\epsilon)/(2\pi)$ is of the order of 100 MHz at T_c and is maximum there (Sec. III B), it lies in a spectral region of the fluctuation dynamics where, close to T_c, the central mode[16,31,32] plays the important role. As shown in Sec. III D, in this region it is given by a Lorentzian with temperature-dependent half-width $\rho \propto \omega_0^2 \propto \chi^{-1}$.[30,31] We then have, close to T_c,

$$S(\vec{q}, \omega) \sim S(\vec{q}, 0)\rho^2/(\rho^2 + \omega^2) . \tag{22}$$

Inserting Eq. (22) into Eq. (10) yields the implicit equation

$$\Delta H^2 \propto \sum_{\vec{q}} \rho S(\vec{q}, 0) \arctan(\omega_1/\rho) , \tag{23}$$

with $\omega_1(\epsilon)$ the frequency equivalent of $\Delta H(\epsilon)$. In the slow-motion regime we have $\omega_1(\epsilon) = \omega_m(\epsilon) \gg \rho(\epsilon)$, yielding the slow-motion expression of Eq. (19). For increasing $|\epsilon|$, $\omega_1(\epsilon)$ and $\omega_m(\epsilon)$ decrease and $\rho(\epsilon)$ increases. For the changeover region where $\omega_1 \simeq \rho$ the arctangent begins to bend off from $\frac{1}{2}\pi$, causing the linewidth to decrease faster with growing $|\epsilon|$, as observed. For higher $|\epsilon|$ the line becomes motionally narrowed. This region is characterized by $\omega_1 < \omega_m \ll \rho$, and Eq. (23) yields the fast-fluctuation solution of Eq. (11). Since $\omega_1(\epsilon)$ decreases and $\rho(\epsilon)$ increases for growing $|\epsilon|$, the temperature region covered by the changeover must be fairly small. As pointed out to us by Rigamonti,[36] the changeover thus arises at that temperature where the central peak half-width becomes of the order of the instantaneous spread in Larmor frequency $\omega_m(T)$. This interpretation allows a direct estimate of the central peak half-width from $\Delta H(T)$ to be of the order of 70 MHz at $T \simeq T_c + 0.8 \pm 0.3$ K, a magnitude which is too low to be resolved by neutron diffraction techniques and has hence been unknown so far. The 50 : 50% relation of Lorentzian to Gaussian type of the resonance at $T_c + 1.5$ K confirms that the changeover occurs near this temperature.

Internal strains and impurities slightly shift the transition temperature,[43] therefore inhomogeneities of these quantities in the crystal may smear out T_c within a limited range. This, together with possible response nonlinearities due to the strong mechanical link between the oxygen octahedra, also cause a lowering of ΔH near T_c. However, such effects yield a round-off resulting in a zero derivative of ΔH with respect to T at T_c, whereas the experiment shows a monotonic increasing derivative down to $T_c + 0.15$ K as predicted by the cusp-shaped behavior. Hence, these influences are restricted to within about 0.1 K in the present experiment. At this temperature the width of the central peak using $\rho = \rho_0 \epsilon^\gamma$ is then about 5 MHz, whereas ω_m is 100 MHz. Thus, there, we are certainly in the slow-motion regime.

F. Remarks on Damping Function Parameters and Refinement of Interpretation

Very recently, Schneider[30] has given within the Mori framework[29] a justification of the form of the complex damping function (5) used, finding $\sigma = 0$, and has shown that the parameters δ^2 and λ are uncritical at T_c. Moreover, he has given an interpretation of these parameters for the case applying to $SrTiO_3$. As was assumed earlier by Shirane and Axe[32] for the case of a transition connected with a soft mode at $\vec{q} = 0$, δ^2 represents the quadratic dif-

ference of high and low frequency response $\delta^2(\vec{q}) = \omega_\infty^2(\vec{q}) - \omega_0^2(\vec{q})$, where ω_0^2 is given by Eq. (3). The static part $S(\vec{q}, \omega = 0)$ needed for the fast-fluctuation regime is then, from Eq. (7),

$$S(\vec{q}, \omega = 0) \propto T\chi^2(\vec{q}, \epsilon)\frac{\delta^2(\vec{q})}{\lambda(\vec{q})} = T\chi^2(\vec{q}, \epsilon)\frac{\omega_\infty^2(\vec{q}) - \omega_0^2(\vec{q})}{\lambda(\vec{q})} . \quad (24)$$

From neutron scattering measurements near the phase transition in Nb_3Sn caused by an acoustic instability it was shown by Shirane and Axe[32] that δ^2 can, to a good approximation, be taken as temperature independent. This has been assumed in the phenomenological treatment of Sec. III A. The treatment could, however, be refined by taking into account a possible weak temperature dependence of δ. For this we set[30]

$$\omega_\infty^2(\vec{q}) = a + b\epsilon^n + \omega_\infty^2(\vec{q} \neq 0) , \quad \omega_0^2(\vec{q}) = c\epsilon^\gamma + \omega_0^2(\vec{q} \neq 0) , \quad (25)$$

where a is the square of the soft-mode frequency at the R corner and $T = T_c$. The exponent n has been determined above T_c to be near unity.[6] From this,

$$\delta^2(\vec{q}) = a + b\epsilon^n - c\epsilon^\gamma + \omega_\infty^2(\vec{q} \neq 0) - \omega_0^2(\vec{q} \neq 0) \simeq a' + b\epsilon - c\epsilon^\gamma . \quad (26)$$

The difference $b\epsilon - c\epsilon^\gamma$ is expected to change sign close to T_c and to be increasingly negative with growing ϵ. This means that not too close to T_c, δ^2 decreases weakly for increasing temperature. Inserting Eq. (26) into Eq. (24) we obtain, from Eq. (11),

$$\Delta H \simeq \tilde{\Delta} H \epsilon^{-\nu(1-2\eta)}[1 - B(\epsilon)] , \quad (27)$$

where $\tilde{\Delta}H$ is constant and the small correction $B(\epsilon)$ vanishing at T_c changes sign close to T_c and is slightly increasing for growing ϵ. It makes the increase of ΔH for $T \to T_c^+$ somewhat stronger and hence may slightly raise the apparent exponent of $\Delta H(\epsilon)$. Therefore, such a weak temperature dependence of δ could be partially responsible for the difference between the experimental exponent "ν" $= 0.74 \pm 0.03$ and the expected value of $\nu \simeq 0.65$ (Sec. III C). If so, the anisotropy parameter Δ describing the $\vec{q}$ anisotropy of the static susceptibility and hence of the correlation may be influenced towards smaller anisotropy.

IV. INTERPRETATION FOR $T \leq T_c$

From Fig. 2 it is seen that the temperature-dependent line broadening at $T_c - \Delta T$ is generally smaller than at $T_c + \Delta T$. Such behavior is related to the general fact that order-parameter fluctuations above a phase transition are larger than below.[23] In terms of a Landau potential[25] this results from the fact that at T_c the potential well is split into two minima at $\pm\varphi_c^0(T)$, implying a larger curvature of the potential well at the minima below than above T_c. Owing to the smaller effect, the experimental temperature dependence of the line broadening below T_c is less accurate than above. Furthermore, since within about 2 K below T_c the linewidth is difficult to define (Sec. II), the broadening cannot be determined in this temperature range.

The general expression for the dynamic form factor $S(\vec{q}, \omega)$ of Eq. (2) is also applicable to the low-temperature phase around the Γ point at $\vec{q} = 0$ of the Brillouin zone. However, in this region the inelastic neutron scattering data[39] do not allow an accurate determination of the calibration parameter κ_0 of the inverse correlation length, although it appears to be of the same order as above T_c. Taking the same value as above and keeping in mind that below T_c the unit cell is doubled, a good fit to the data in the temperature range from 90 to 103 K is obtained from Eq. (13) with $\nu' = 0.65$ and Δ of the order of $\frac{1}{25}$ (Fig. 7). However, owing to the scattering of the data, Δ is only defined within about a factor of 4, and an independent determination of ν' and Δ is not possible. This fit, however, means that the behavior of the parameters characterizing the static part of $S(\vec{q}, \omega)$ does not appear to change very significantly from above to below T_c. Such a change would, in principle, be possible, since the crystal symmetry is altered and the soft mode, below T_c at $\vec{q} = 0$, couples to different modes. This fitting shows further that the static scaling hypothesis[23] yielding $\nu = \nu'$ is obeyed within our experimental accuracy. The mean slope of Fig. 7 corresponds to an apparent exponent of -0.88 ± 0.08.

The ratio of $\Delta H(\epsilon)/\Delta H(-\epsilon)$ is, for all temperatures, larger than unity and varies between 2 and 3 in the temperature range investigated. This ratio in the fast-fluctuation regime is seen from Eqs. (3), (7), (11), and (13) to depend on the ratios

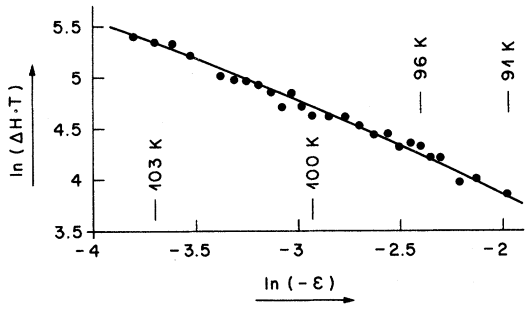

FIG. 7. Comparison between experiment and theory for the φ_c-broadened linewidths below T_c. The solid line is calculated from Eq. (13) with $\nu' = 0.65$, $\Delta = 0.04$. For κ_0 the same value as used above T_c has been taken.

of $\chi(\vec{q}, \epsilon)$, the real part of the damping function $\Gamma(\vec{q}, \omega=0)$, κ_0, Δ, and the proportionality constant between $\omega_0^2(\vec{q}, \epsilon)$ and $\chi(\vec{q}, \epsilon)$. Since no theoretical or experimental values for these ratios are available, the experimental ratio $\Delta H(\epsilon)/\Delta H(-\epsilon)$ cannot be analyzed numerically. Qualitatively again, the experimental value larger than unity reflects the fact that the fluctuations of the order parameter are larger above than below T_c.

V. INTERPRETATION OF ANISOTROPY IN LINEWIDTH

As seen from Fig. 4, for $T < 115$ K the experimental linewidth is anisotropic for the magnetic field along [110] and [101]. In Sec. II it was shown that with the former direction of $\vec{H}$ one measures the fluctuations around the low-temperature domain axis (denoted by φ_c in Fig. 4), and for the latter those around an axis perpendicular to it (called φ_a fluctuations in Fig. 4). This anisotropy is *a priori* not surprising for $T < T_c$ since there the crystal symmetry is tetragonal and hence the two directions are no longer equivalent. For $T \geq T_c$, however, the crystal is cubic, and the observed anisotropy is qualitatively not explainable by static symmetry properties of the crystal.

A. Interpretation for $T \geq T_c$

Above T_c, the φ_c-broadened linewidth ΔH_c is larger than the corresponding φ_a-broadened width ΔH_a. The ratio $\Delta H_c/\Delta H_a$ increases for $T \to T_c^+$ and reaches its maximum value of about 3 at T_c (Fig. 5). If for both the φ_c and φ_a fluctuations the linewidth at T_c is dominated by the slow-motion regime, the square of this value gives the ratio of $\langle\varphi_c^2\rangle/\langle\varphi_a^2\rangle$ at the phase transition [Eqs. (9) and (18)]. Owing to the cubic point symmetry of the crystal this anisotropy is dynamical and must be connected with growing regions of correlated rotational fluctuations. Only for temperatures close enough to T_c are these regions significantly larger than a few unit cells. Their size is given by the correlation length $\xi(\epsilon) \equiv 1/\kappa(\epsilon)$ which at 115 K is of the order of five unit cells.[16] Within a certain region, the local fluctuations pertaining to one particular component of the three equivalent $\varphi^{\langle 100\rangle}$ rotations are correlated in the sense of the low-temperature tetragonal phase. The dynamic symmetry in this region is therefore no longer cubic since one of the three $\langle 100\rangle$ axes is distinguishable from the other two. This is the axis of correlated rotations. Hence, owing to the dominance of one particular c-type correlation, the crystal "feels" the low-temperature phase. The correlation with respect to that local fluctuation component α means that within the correlation region the static susceptibility $\chi^{\alpha\alpha}(\vec{q}, \epsilon) \sim 1/(\vec{q}^2 + \kappa^2)$ is no longer equal for the other two components α, but is larger for the correlated component, since its κ is smallest.

In the sample transforming below T_c into a monodomain with c axis along [001], the correlations above T_c will occur predominantly with respect to the $\varphi^{[001]}$ fluctuations. It is with respect to these fluctuations that the correlation length will diverge, since this type of rotation is the order parameter of the sample below T_c. For the fluctuations around [100] and [010] the correlation length will remain finite. These motions are of quasi-order-parameter type. From Eq. (13) it is seen that for the fast-motion regime the line broadening is directly related to the temperature behavior of the inverse correlation length $\kappa(\epsilon)$ connected with the particular fluctuation component under investigation. The anisotropy in linewidth displayed in Fig. 4 hence reflects the different increase in correlation length for the two kinds of fluctuations within the correlated pancake-type areas. This difference becomes significant when the correlation range of $\varphi^{[001]}$ fluctuations grows larger than a few unit cells. This is the case for temperatures below 115 K, as noted above.

$\Delta H_a(T)$ is shown in Fig. 8 on a log-log scale, using the same background as in Fig. 2(c). The apparent negative exponent given by the slope for $T < 115$ K of about 0.55 is smaller than in the ΔH_c case, and the curve appears to bend off around 107.5 K. This indicates a slower than simple exponential increase of ξ for $T \to T_c^+$. Close to T_c, for this case ξ probably behaves in a cusp-like way, but a quantitative analysis is not meaningful owing to the changeover to the slow-fluctuation regime, which in this case may be different.

The observed anisotropy cannot be caused by an anisotropic transverse local mode of the Fe^{3+}-V_O center. Such a possibility exists in principle because for the ΔH_c measurements the center axes are perpendicular to the axis of the φ_c fluctuations, whereas for the φ_a width ΔH_a they are parallel to it. This results in an orthorhombic and axial local symmetry, respectively. The influence of

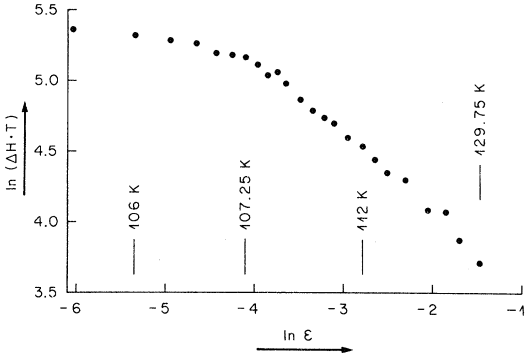

FIG. 8. Log-log plot of the temperature-dependent line-broadening caused by φ_a fluctuations in a monodomain sample for $T \geq T_c$.

local-mode anisotropy is excluded by comparison of the φ_a linewidth with that of another φ_a broadened line whose centers "see" the same orthorhombic local symmetry as in the φ_c case. This line is the other axial line with $\vec{H}$ near [101] (cf. Sec. II). It becomes the "m" line below T_c (see I) in the "monodomain" sample used. Its resonance field is sensitive to φ_c^2, whence the broadening by φ_c fluctuations is negligible. The width of this line for $T \geq T_c$ is found to be equal to the width of the other φ_a-broadened line within the experimental error. This equality for centers with orthorhombic and axial local symmetry, respectively, would be an extraordinary coincidence if the linewidth anisotropy were due to an anisotropic local mode. Furthermore, neither would the inversion of the anisotropy below T_c be consistent with such an explanation. Hence, the anisotropic width above T_c is due to anisotropic φ^a-fluctuations.

B. Interpretation for $T \leq T_c$

Below T_c, the φ_a-broadened linewidth is observed to show a practically symmetric behavior with respect to T_c in contrast to the φ_c-broadened width (Fig. 4). This corresponds to the fact noted previously that the φ_a rotations do not provide the generalized order parameter below T_c. This means that $\langle \varphi_a \rangle$ is zero also in the low-temperature phase. In terms of a Landau potential, [25] this in turn implies that the potential well around $\varphi_a = 0$ is not split at T_c into two minima at $\pm \varphi_a^0(T)$ as is the case for the φ_c-type motions. Instead, its curvature will simply pass through a minimum value at T_c corresponding to a maximum in fluctuations. Below T_c it will be smaller than the curvature of the split φ_c potential well at the two minima. This gives rise to the two distinct soft-mode branches observed below T_c, [5,6] the doubly degenerate φ_a mode being lower in frequency than the singly degenerate φ_c mode. This feature further implies the φ_a fluctuations to be larger than the φ_c-type ones. Both effects broaden the φ_a line more than the φ_c line, in agreement with experiment. A meaningful quantitative analysis is made difficult for similar reasons as above T_c, the behavior of the correlations as well as of the central mode for the φ_a fluctuations being unknown, i.e., the anisotropy of the central mode. Furthermore, from Fig. 4 it results that also the background width becomes markedly anisotropic for $T \to 0$ K. This makes an accurate determination of the net broadening uncertain. The reason for the relatively strong and increasing anisotropy of background width is probably an anisotropy of the ferroelectric mode below about 50 K. [44] For the experimental arrangements chosen, the anisotropy of fluctuations of Fe^{3+} position, owing to an anisotropic ferroelectric mode, should not be reflected in the linewidths. However, the increasing anisotropic polarization fluctuations of decreasing frequency yield a larger broadening for the φ_a line, as observed.

VI. DISCUSSION

A. Comparison with Other Experiments

In agreement with our quantitative analysis yielding two-dimensionally anisotropic correlations are the critical anisotropic x-ray diffusive scattering data of Denoyer and Lambert[45] in $KMnF_3$ and $NaNbO_3$. $KMnF_3$ undergoes an isomorphic phase transition to $SrTiO_3$ at 184 K, [46] whereas for the cubic-to-tetragonal phase transition in $NaNbO_3$ at ~ 915 K it is driven by a soft M-point phonon [$q_M = (\frac{1}{2}, \frac{1}{2}, 0)(2\pi/a)$]. [56] The two-dimensional correlation anisotropy in $KMnF_3$ tends to increase for $T \to T_c$. [47] If this behavior is also valid in $SrTiO_3$ it implies that the bend off of $\Delta H(T)$ from the theoretical curve at 107 K (Fig. 6) is really due to the changeover to slow fluctuations and does not mean that the correlation gets more three dimensional.

A fairly direct proof of the two-dimensional anisotropy in the susceptibility $\chi(\vec{q}, \epsilon)$ is obtained from the anisotropic dispersion of the soft mode around the R corner. In $KMnF_3$ this dispersion is completely flat between the R and M points of the Brillouin zone. [48] The softening of nearly the entire branch between these two points is responsible for the fact that some 100 K below the $O_h^1 \to I4/mcm$ phase transition at 184 K the crystal undergoes a second phase transition connected with a softening of the M-point mode. [46] It indicates that the rotational motions above 184 K are practically completely uncorrelated from plane to plane. The situation is somewhat less dramatic in $SrTiO_3$, although the dispersion anisotropy is still very pronounced. Recent neutron-diffraction measurements by Stirling and Cowley[40] have shown that in this crystal the dispersion parameter b as defined by

$$\omega^2(\vec{q}) = \omega_R^2 + b\vec{q}^2 \tag{28}$$

is about 8 times larger for $\vec{q}$ progressing from R to Γ than from R to M. Here again the origin of q space is taken at the R corner, and ω_R denotes the soft-mode frequency at the R point. From this data an estimate of the $\vec{q}$ anisotropy of $\chi(\vec{q}, \epsilon)$ can be made by the relation

$$\chi(\vec{q}, \epsilon) = \frac{\chi_0}{\vec{q}^2 + (1-\Delta)q_z^2 + \kappa^2} \propto \frac{1}{\omega_0^2(\vec{q})} \simeq \frac{1}{\omega^2(\vec{q})}, \tag{29}$$

with $\omega^2(\vec{q})$ given by Eq. (28), and q_z pointing from R to M along the c axis. For T close to T_c, where $\omega_R^2 \simeq 0$ and $\kappa^2 \simeq 0$, one obtains $\Delta \simeq 0.08$, which is comparable to the value found here and again proves the non-negligible anisotropy of the correlation.

Recently, Bonera, Borsa, and Rigamonti[49] re-

ported on strongly temperature-dependent direct nuclear Na^{23} relaxation near T_c in $NaNbO_3$. Since, owing to its symmetry, the q_R soft mode does not couple linearly to the electric field gradient (EFG) at the Na site, it does not contribute to the direct relaxation process. The symmetry of the q_M mode, however, implies a linear coupling to the EFG. The relaxation rate is proportional to the spectral density of the fluctuations at the Larmor frequency ω_L of the nuclear spins,[49] which lies very close to zero compared to the usual phonon frequencies. The relaxation time of the Na^{23} nuclei can thus be significantly shortened only by a critical slow-down of the modes around q_M, especially when this slow-down is connected with an increasing central peak. The strongly increasing relaxation rate at T_c in $NaNbO_3$ can thus be explained in terms of a soft M-point phonon. If the transition is driven by a soft R-corner mode it must, as assumed in Ref. 49, be connected with a practically completely uniform softening of the entire branch between the R and M points, corresponding to a strong decorrelation of NbO_6 octahedra rotation from plane to plane. This situation corresponds to the one in $KMnF_3$. Since in $SrTiO_3$ the dispersion between R and M is not entirely flat and the q_M phonon frequency lies near 8 meV at T_c,[40] the relaxation of Sr^{87} nuclei is not critically enhanced near T_c, as observed by Angelini, Bonera, and Rigamonti.[50] Nevertheless, the correlation is significantly two-dimensional.

In agreement with the present observation of anisotropic fluctuations $\langle\varphi_a^2\rangle$ and $\langle\varphi_c^2\rangle$, also for temperatures slightly above T_c, are very recent optical birefringence measurements in $SrTiO_3$ by Courtens.[51] They were carried out on one of the "monodomain" samples used here and show, besides a systematic decrease of birefringence Δn on approaching T_c^-, a tail within a comparable temperature region above T_c and a small but distinct peak at the transition temperature. The birefringence is $\Delta n = S(\langle\varphi_c\rangle^2 + \langle\delta\varphi_c^2\rangle - \langle\varphi_a^2\rangle)$, S being a proportionality constant. Owing to the entirely different characteristic frequency these experiments "see" the fluctuations as static for *all* temperatures. Well below T_c, $\langle\delta\varphi_c^2\rangle < \langle\varphi_a^2\rangle$, and the birefringence deviates systematically to smaller values from the static value of $\langle\varphi_c\rangle^2$ determined by EPR.[11] For $T \to 0$, both $\langle\delta\varphi_c^2\rangle$ and $\langle\varphi_a^2\rangle$ are small, which allows us to obtain the proportionality constant S using the EPR result. With this value of S, the peak of Δn at T_c was computed,[51] inserting into the expression $\Delta n = S(\langle\delta\varphi_c^2\rangle - \langle\varphi_a^2\rangle)$ the fluctuation values given in Fig. 4 of the present paper. This is permissible since at T_c the EPR linewidth is given by quasistatic fluctuation values. The Δn value which is obtained in this way agrees quantitatively with the peak in Δn found experimentally. This confirms by an independent experiment an essential result of the present investigation. The observation of a tail ($\Delta n \neq 0$) for $T > T_c$ also yields an anisotropy in fluctuations $\langle\varphi_c^2\rangle \gg \langle\varphi_a^2\rangle$, in agreement with our conclusions. The critical exponents β and ν obtained from birefringence experiments are also comparable with those derived in the present paper. Differences between a- and c-type fluctuations have been observed for the anisotropic antiferromagnet MnF_2 by inelastic neutron scattering.[52]

Recently, a paramagnetic defect was analyzed by EPR in neutron-irradiated $SrTiO_3$ by Schirmer and Müller.[53] It results from a Ti^{3+} ion on a Sr^{2+} site lying "off center" by 0.03 Å. This center shows axial symmetry in the cubic phase for temperatures well above T_c and an orthohombic one for $T < T_c$, and both centers are observed simultaneously for temperatures slightly above T_c. The components of the tetragonal center are the averages of the orthorhombic ones. The orthorhombicity is caused by the tilting of the oxygen octahedra, but does not follow the order parameter in a continuous way. The off-center Ti^{3+} rather sticks to the nearest oxygen if the fluctuations last longer than $\tau \simeq 10^{-9}$ sec, whereas for shorter fluctuations the averaged spectrum results. For a temperature range of about 40 K above T_c, orthorhombic spectra are still seen, indicating that fluctuations slower than 10^{-9} sec with sufficient amplitude are still present. It has been found theoretically,[30,31] and can be deduced from Eq. (2) (see Sec. III D), that the width of the central peak has a temperature dependence of ϵ^{γ}. Thus at $T - T_c = 40$ K the width is computed to be approximately $70 \times 10^6 (40)^{\gamma} = 8 \times 10^9$ Hz, a value compatible with the observation of sizeable oscillator strength in the range near 10^9 Hz.

The present investigation of dynamical properties of $SrTiO_3$ indicates validity of the critical exponent ν in large temperature regions at least above T_c. Similar behavior has been observed in the birefringence measurements by Courtens,[51] as well as in Rayleigh scattering experiments in CO_2 (Ref. 54) and in the temperature dependence of the liquid-gas density differences of several fluids.[55] Below T_c, the accuracy for $T < 100$ K is too small to allow a possible detection of a changeover to a classical region as observed for the static-order-parameter measurements.[11] However, the range of ν and β may not correlate.

B. Dependence of Experimental Linewidth on Line Shape

As mentioned in Sec. II, the experimental linewidth was taken as the peak-to-peak separation of the absorption derivative being equal to the separation of the absorption-curve inflection points. For a fixed line shape this is proportional to the width at half intensity $\Delta H_{1/2}$ given by $\Delta H_{1/2}^L = 1.73\,\Delta H_{\text{expt}}$, and $\Delta H_{1/2}^G = 1.18\,\Delta H_{\text{expt}}$ for Lorentzians and Gaussians, respectively. When the Lorentzian shape for

$T \to T_c$ changes to Gaussian, the difference in proportionality factors would result in an apparently too large increase of the linewidth. This effect, however, is counterbalanced by the linear subtraction of the Lorentzian background width. This procedure is exactly correct only for a convolution of two Lorentzians, whereas if one or both constituents are partly Gaussian-like, it produces too small linewidths. Numerical estimates show the two effects to cancel within a few percent for the linewidths observed in the fast-motion regime.

ACKNOWLEDGMENTS

The authors are indebted to F. Borsa, R. Cowley, F. Schwabl, and especially to A. Rigamonti for communicating to us their unpublished results and for pertinent suggestions on this work, as well as to H. Thomas, R. Comes, E. Courtens, J. Feder, P. Hohenberg, J. Jacrot, W. Känzig, M. Lambert, E. Pytte, T. Riste, T. Schneider, and H. E. Stanley for valuable discussions and comments.

[1]K. A. Müller, Helv. Phys. Acta 31, 173 (1958).

[2]L. Rimai and G. deMars, Phys. Rev. 127, 702 (1962).

[3]H. Unoki and T. Sakudo, J. Phys. Soc. Japan 23, 546 (1967).

[4]K. A. Müller, W. Berlinger, and F. Waldner, Phys. Rev. Letters 21, 814 (1968).

[5]P. A. Fleury, J. F. Scott, and J. M. Worlock, Phys. Rev. Letters 21, 16 (1968).

[6]G. Shirane and Y. Yamada, Phys. Rev. 177, 858 (1969).

[7]B. Alefeld, Z. Physik 222, 155 (1969).

[8]R. O. Bell and G. Rupprecht, Phys. Rev. 129, 90 (1963).

[9]W. Kaiser and R. Zurek, Phys. Letters 23, 668 (1966).

[10]B. Berre and K. Fossheim, Phys. Rev. B 5, 3292 (1972).

[11]K. A. Müller and W. Berlinger, Phys. Rev. Letters 26, 13 (1971).

[12]K. A. Müller, *Structural Phase Transitions and Soft Modes*, edited by E. J. Samuelsen, E. Andersen, and J. Feder (Universitetsforlaget, Oslo, Norway, 1971), p. 85.

[13]Th. von Waldkirch, K. A. Müller, W. Berlinger, and H. Thomas, Phys. Rev. Letters 28, 503 (1972).

[14]E. S. Kirkpatrick, K. A. Müller, and R. S. Rubins, Phys. Rev. 135, A86 (1964).

[15]Over the same temperature range, M. Capizzi and A. Frova probably observed an enhanced optical electronic absorption (unpublished).

[16]T. Riste, E. J. Samuelsen, K. Otnes, and J. Feder, Solid State Commun. 9, 1455 (1971).

[17]Th. von Waldkirch, K. A. Müller, and W. Berlinger, Phys. Rev. B 5, 4324 (1972).

[18]K. A. Müller, W. Berlinger, M. Capizzi, and H. Gränicher, Solid State Commun. 8, 549 (1970).

[19]*Dial-A-Volt*, General Resistance Inc., New York, N. Y.

[20]K. A. Müller and W. Berlinger, Phys. Rev. Letters 29, 715 (1972).

[21]G. Bonera, F. Borsa, and A. Rigamonti, Nuovo Cimento Suppl. (to be published).

[22]*Spin-Lattice Relaxation in Ionic Solids*, edited by A. A. Manenkov and R. Orbach (Harper, New York, 1966).

[23]H. E. Stanley, *Introduction to Phase Transitions and Critical Phenomena* (Clarendon, Oxford, England, 1971).

[24]W. Cochran and A. Zia, Phys. Status Solidi 25, 273 (1968).

[25]J. C. Slonczewski and H. Thomas, Phys. Rev. B 1, 3599 (1970).

[26]E. Pytte and J. Feder, Phys. Rev. 187, 1077 (1969); J. Feder and E. Pytte, Phys. Rev. B 1, 4803 (1970).

[27]H. Thomas and K. A. Müller, Phys. Rev. Letters 21, 1256 (1968).

[28]K. A. Müller, W. Berlinger, and J. C. Slonczewski, Phys. Rev. Letters 25, 734 (1970).

[29]Equation (2) can, for instance, be derived from Mori's theory on correlation functions [H. Mori, Progr. Theoret. Phys. (Kyoto) 34, 399 (1965)].

[30]T. Schneider, Phys. Rev. B (to be published).

[31]F. Schwabl, Phys. Rev. Letters 28, 500 (1972).

[32]G. Shirane and J. D. Axe, Phys. Rev. Letters 27, 1803 (1971). In this note, the *Ansatz* refers to a soft acoustic mode rather than to an optic one as in our case and is more straightforward to be justified.

[33]The dynamic form factor does not obey the dynamical scaling hypothesis.

[34]Equation (8) indicates that δH is proportional to the *local* $\varphi_{\vec{q}}$. Therefore, the proportionality constant A stands outside the summation over $\vec{q}$ and hence does not depend on $\vec{q}$, in contrast to NMR relaxation (Ref. 21) or the NMR-linewidth measurements by A. M. Gottlieb and P. Heller [Phys. Rev. B 3, 3615 (1971)].

[35]A. Abragam, *The Principles of Nuclear Magnetism* (Clarendon, Oxford, England, 1961), Chap. 10.

[36]A. Rigamonti (private communication).

[37]The increasing background width below 50 K can be caused by increasing influence of dipolar interaction with Fe^{2+} ions [A. M. Stoneham, K. A. Müller, and W. Berlinger, Solid State Commun. 10, 1005 (1972)], or by the softening of the ferroelectric mode as discussed in Sec. V.

[38]T. Schneider and E. Stoll, in Ref. 12, p. 383.

[39]T. Riste, E. J. Samuelsen, and K. Otnes, in Ref. 12, p. 395.

[40]W. G. Stirling and R. A. Cowley (private communication).

[41]H. E. Stanley, in Ref. 12, p. 271.

[42]The dependence on the correlation length inferred from Eq. (13) results from the κ dependence of the susceptibility $\chi(\vec{q}, \epsilon)$ and hence reflects the increasing magnitude of the fluctuations for $T \to T_c$.

[43]B. Pietrass and E. Hegenbarth, Phys. Status Solidi 34, K119 (1969); D. W. Deis, M. Ashkin, J. K. Hulm, and C. K. Jones, Bull. Am. Phys. Soc. 15, 102 (1970).

[44]T. Sakudo and H. Unoki, Phys. Rev. Letters 26, 851 (1971).

[45]F. Denoyer and M. Lambert, J. Phys. (Paris) 33, C2, 131 (1972).

[46]V. J. Minkiewicz and G. Shirane, J. Phys. Soc. Japan 26, 674 (1969).

[47]F. Denoyer, R. Comes, and M. Lambert (private communication).
[48]G. Shirane, in Ref. 12, p. 217.
[49]G. Bonera, F. Borsa, and A. Rigamonti, J. Phys. (Paris) 33, C2-195 (1972).
[50]G. Angelini, G. Bonera, and A. Rigamonti, *XVIIth* Congress Ampere (Turku, Finland, 1972).
[51]E. Courtens, Phys. Rev. Letters 29, 1380 (1972).
[52]M. P. Schulhof, R. Nathans, P. Heller, and A. Linz, Phys. Rev. B 4, 2254 (1971).
[53]O. F. Schirmer and K. A. Müller, Phys. Rev. B (to be published).
[54]J. A. White and B. S. Maccabee, Phys. Rev. Letters 26, 1468 (1971); B. S. Maccabee and J. A. White, Phys. Rev. Letters 27, 495 (1971).
[55]E. A. Guggenheim, J. Chem. Phys. 13, 253 (1945); see also Ref. 23, p. 10.
[56]*Reference added in proof.* A. M. Glazer and H. D. Megav, Phil. Mag. 25, 1119 (1972).

PHYSICAL REVIEW B VOLUME 7, NUMBER 3 1 FEBRUARY 1973

Specific Heats of Dilute Magnetic α-Phase Cu-Au(Fe) Alloys*

W. C. Delinger,† W. R. Savage, and J. W. Schweitzer
Department of Physics and Astronomy, The University of Iowa, Iowa City, Iowa 52240
(Received 21 August 1972)

This study of the specific heats of dilute magnetic α-phase Cu-Au(Fe) alloys is a continuation of our work on dilute Fe in binary-host alloys. Our previous specific-heat results for the α-phase Cu-Al(Fe) system indicated that the Kondo effect depended on the particular local environment of the Fe impurity. The present study was motivated by resistivity experiments which suggested for Cu-Au(Fe) a contrasting picture where local-environment effects are not important. The specific heats of a series of α-phase Cu-Au and dilute magnetic Cu-Au(Fe) alloys with Fe concentrations near 0.04 at.% were measured over the temperature range 1–10 K. The alloys had Au concentrations of 2.4, 4.8, and 10 at.%. The excess specific heat due to the Fe impurities show a broad peak characteristic of the Kondo effect. A recently derived theoretical expression for the Kondo effect in the specific heat was successful in fitting these Cu-Au(Fe) results and the Cu(Fe) results of other investigators. The contribution from the Fe impurities for the various alloys had the same functional dependence on a scaled temperature T/T_K, where the T_K decreased with increasing Au concentration. This agreed with the existence of a universal resistance curve for Cu-Au(Fe) found by other experimenters. Comparisons are made with our previous specific-heat result for the Cu-Al(Fe) system which could not be fit with a universal curve. It is suggested that local-environment effects are important in the Cu-Al(Fe) system in contrast with the Cu-Au(Fe) system.

I. INTRODUCTION

The study of the Kondo effect associated with dilute magnetic impurities in binary-host alloys is of special interest since it yields information not only on the Kondo effect but also on the electronic properties of the host alloy. Most current theories of the Kondo effect based on simple model Hamiltonians suggest that the Kondo effect due to a magnetic impurity depends on a single characteristic temperature parameter T_K, the Kondo temperature. Resistivity measurements by Loram *et al.*[1] demonstrated that the excess resistivity of Cu-Au(Fe) due to the Fe impurities could be fit to a universal function of T/T_K where T_K decreased rapidly with increasing Au concentration. The existence of such a universal curve is a significant experimental observation. It gives confidence in the possible quantitative applicability of simple one-parameter models, such as the Kondo model, to real systems for a rather large range of the parameter. However, one expects that in the case of a binary-host alloy it is necessary to take into account the possibility that the parameter T_K will depend on the particular local environment of the impurity. Local variations in the density of states will produce local variations in T_K. If these local variations are large, one would not expect to find the macroscopic measurements in agreement with a universal curve. Indeed Zrudsky and the present authors[2] found that the excess specific heats of dilute magnetic α-phase Cu-Al (Fe) alloys could not be fit by a universal curve. This contrasting behavior between the specific heat of Cu-Al (Fe) and the resistivity of Cu-Au(Fe) motivated the present study of the specific heat of the Cu-Au(Fe) system.

The specific heats of a series of α-phase Cu-Au and dilute magnetic Cu-Au(Fe) alloys with Fe concentrations near 0.04 at.% were measured over the temperature range 1–10 K. The alloys had Au concentrations of 2.4, 4.8, and 10.0 at.%. The excess specific heat due to the Fe impurities showed the broad anomaly characteristic of the Kondo effect. This contribution for the various alloys could be fit to the same functional dependence on a scaled temperature T/T_K where T_K decreased with increasing Au concentrations. Therefore the specific-heat results for the Cu-Au